Ultra high-performance fiber reinforced concrete panel subjected to high velocity impact

V.C. Mai*ᵃ ⓘD **, X.B. Luuᵃ, V.T. Nguyenᵇ**

ᵃ *Kumoh National Institute of Technology, Gumi, Gyeongbuk, South Korea*

ᵇ *Institute of Techniques for Special Engineering, Le Quy Don Technical University, Ha Noi, Viet Nam*

*E-mail: maivietchinh@lqdtu.edu.vn

Abstract. In the last few decades, several full-scale tests have been performed to study the behavior of Ultra High-Performance Fiber Reinforced Concrete (UHPFRC). However, only limited research has been devoted to simulate performance of UHPFRC subjected to special load and impact, such as high-velocity impact. Accurate modeling and simulation of the UHPFRC panel subjected to high velocity impact is a big challenge involving costly experimental characterization of material and verification of ballistic impact response with actual test data. This article investigates the dynamic behavior of UHPFRC panel against multiple bullet impacts using the Holmquist-Johnson-Cook damage model incorporating both the damage and residual material strength. The projectile used in this study is chosen with high-speed and low-weight like the fragments which can be formed by industrial accidents or in an explosion. The kinetic and internal energies of the UHPFRC panel are also evaluated. The analysis results are compared to the High Strength Concrete (HSC) in terms of capability to absorb energy and reduce the damage on target panel.

1. Introduction

Invented about three decades ago, the so-called ultra-high performance concretes (UHPC) result in high compressive strength values of 150 N/mm² and more [1]. UHPC is characterized by steel fibers, cement, silica fume, fine sand, super plasticizer, and very low water-cement ratio. UHPC possesses very high compressive strength, good tensile strength, enhanced toughness, and durability properties in comparison to conventional concrete [2–8]. However, one of the main drawbacks of UHPC is its brittleness property. To overcome brittleness of UHPC, fibers are often added to UHPC and this type of concrete is referred to as Ultra High-Performance Fiber Reinforced Concrete (UHPFRC). The inclusion of reinforcement fibers in UHPC improves its mechanical properties, reduces its brittleness, and alters the crack propagation behaviors [9]. The UHPC has high compressive and tensile strengths compared to normal or high performance concretes, including good durability due to the combination of the optimum packing density [10]. It is well known that high strength and fiber reinforced concrete (FRC) has good capacity to absorb impact energy [11]. However, compared to conventional concrete, several authors suggested that UHPFRC has much greater capability to absorb energy [12–15]. In addition, UHPFRC can significantly improve impact resistance of cladding panels and walls while maintaining its standard thicknesses and appearance [16]. Such advantages of UHPFRC give the potential to be used for some constructions like military structures or multipurpose complex subjected to the special load like projectile impact. In a broad sense, the projectile impact might be understood as a fragment generated from a high-speed rotating machine in industrial accidents or generated from a direct armed attack [16].

Due to the high technical requirements, high costs of manufacturing UHPFRC, and the security restrictions required for full-scale velocity impact tests, experimental studies on UHPFRC members under

high-velocity impact are very limited. Moreover, UHPFRC is still a type of advanced concrete, and most investigations on its characteristics are predominantly quasi-static. Radoslav Sovják et al., 2013, took the experimental Investigation of UHPFRC Slabs Subjected to Deformable Projectile Impact [17]. Several UHPFRC mixtures with different content of fibers were subjected to deformable projectile impact. A test with an ogive-nose projectile at average velocity shows that the plain UHPC specimen failed in a brittle manner, which makes the slab split into several pieces. Experimental results indicate that the implementation of high-strength steel microfibers significantly increased the resistance to projectile impact. It was stated that UHPFRC has much better resistance to projectile impact in comparison to conventional FRC. Erzar et al., 2017, has led an experimental and numerical research program in collaboration with French universities to evaluate the vulnerability of UHPFRC infrastructure to rigid projectile penetration [16]. They used the concrete model developed by Pontiroli, Rouquand and Mazars (PRM model), especially to take into account the contribution made by the fibers in the tensile fracture process. The collected result was significant, however, the PRM model is based on an isotropic formulation and the fiber ratio actually contributing to the material resistance needs to be more accurately determined. Sebastjan Kravanjaa, Radoslav Sovjákb, 2018, implemented cratering experiments, where the response of the Ultra-High Performance Fiber-Reinforced Concretes with various fiber volume fractions to the high- velocity projectile impact loading was investigated. Based on the experiment results, the increment of the fiber volumetric fraction did not have a significant influence on the depth of the penetration [18]. However, it plays an important role in reducing the crater area and volume. Jianzhong Lai et al., 2018, modeled the Ultra-High-Performance Concrete Subjected to Multiple Bullet. In this study, ultra-high-performance concrete (UHPC) was reinforced by hybrid fibers and corundum aggregates. The effects of hybrid fibers and corundum aggregates on bullet penetration depth and damage to UHPC subjected to multiple bullet impacts were researched. As a result, an empirical model was proposed to predict bullet penetration depths in UHPC based on the formula developed by Gomez [19].

This paper contributes to the development of UHPFRC and its application in the field, where high-impact energy absorption capacity is required. In this paper, a numerical model to predict the impact behavior of a UHPFRC panel penetrated by an ogive-nosed steel projectile is implemented. Due to the relatively high cost of large-scale experimental research, a means of modeling UHPFRC panel under impact load using a computer-aided program is needed to broaden the current knowledge. The numerical simulations were conducted using the ABAQUS software, which is a general FE analysis package for modeling the nonlinear mechanics of structures and their interactions. ABAQUS is based on implicit and explicit numerical methods for problems associated with large deformation and multi-loading environments. The UHPFRC panel has dimensions of 300 mm × 150 mm × 50 mm. The behavior of the UHPFRC panel is modeled using the Holmquist-Johnson-Cook damage model incorporating both the damage and residual material strength. The steel projectile has a small mass and a length of 26.6 mm, and is modeled as a deformable element under an impact velocity of 540 m/s. A general contact surface with nodal erosion is adapted to simulate the contact between the projectile and UHPFRC panel to be more appropriate. Accurate simulation of the structural response to such projectile impact using the Holmquist-Johnson-Cook damage model is a convenient way to radically decrease the cost of efforts relating to the field experiments. The model was also calculated with high strength concrete (HSC) and the results were also compared with UHPFRC to clarify the advantages of UHPFRC compared to conventional concrete under impact effect.

2. Materials and Methods

In terms of the existing dynamic constitutive model, the Holmquist-Johnson-Cook (HJC) model [20] represents a good compromise between simplicity and accuracy for large-scale computations, and has been implemented in ABAQUS for numerical simulations. The HJC model with damage is useful when modeling brittle materials subjected to large pressures, shear strain and high strain rates. The HJC model assumes that the damage variable increases progressively with plastic deformation. This model similarly consists of three components: strength, damage and pressure. The equivalent strength of material is expressed as a function of the pressure, strain rate and damage:

$$\sigma^* = \left[A(1-D) + BP^* \right] \cdot \left(1 + C \, ln \, \dot{\varepsilon}^* \right) \tag{1}$$

Where: P^* denotes the normalized pressure, shown as $P^* = P / f'_c$;

P denotes pressure;

f'_c is the quasi-static uniaxial compressive strength;

$\overset{\bullet}{\varepsilon}{}^{*}$ is the dimensionless strain rate, given by: $\overset{\bullet}{\varepsilon}{}^{*} = \overset{\bullet}{\varepsilon} / \overset{\bullet}{\varepsilon}_O$;

$\overset{\bullet}{\varepsilon}$ is the actual strain rate;

$\overset{\bullet}{\varepsilon}_O$ is the reference strain rate;

D $(0 \leq D \leq 1)$ denotes the damage parameter. Additionally $A, B, N,$ and C denote the material parameters.

The model accumulates damage both from equivalent plastic strain and plastic volumetric strain, and is expressed as:

$$D = \sum \frac{\Delta \varepsilon_P + \Delta \mu_p}{\varepsilon^f + \mu_p^f} \tag{2}$$
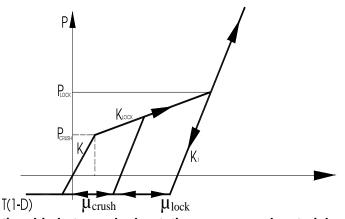
Where:

$\Delta \varepsilon_p, \Delta \mu_p$ are the equivalent plastic strain increment and plastic volumetric strain increment, respectively, during one cycle integral computation;

$\varepsilon_p^f + \mu_p^f$ is the plastic strain to fracture under a constant pressure, which can be expressed as follows:

$$\varepsilon_p^f + \mu_p^f = D_1 \left(P^* + T^* \right)^{D_2} \tag{3}$$

Where:

D_1 and D_2 represent damage constants, and $T^* = T / f'_c$ is the normalized largest tensile strength (T represents the maximum tensile stress).

Figure 1. The relationship between hydrostatic pressure and material volumetric strain.

The equation of state of this model describes the relationship between hydrostatic pressure and volume. The loading and unloading process of concrete can be divided into three response regions. The first zone is the linear elastic zone, where the material is in elastic state. The elastic bulk modulus is given by:

$$k = \frac{P_{crush}}{\mu_{crush}} \tag{4}$$

Where:

P_{crush} and μ_{crush} represent the pressure and volumetric strain arising in a uniaxial compression test. Within the elastic zone, the loading and unloading equation of state is given by:

$$P = k\mu \tag{5}$$

Where:

μ is density parameter: $\mu = \rho / \rho_0 - 1$;

ρ is the current density and ρ_0 denotes the reference density.

The second zone arises at $P_{crush} < P < P_{lock}$, where the material is in the plastic transition state. In this area, the concrete interior voids gradually reduce in size as the pressure and plastic volumetric strain increase. The unloading curve is solved by the difference from the adjacent regions. The third area defines the relationship for fully dense material. The concrete has no air voids. The relationship between pressure and the volumetric strain is given by:

$$P = k_1 \overline{\mu} + k_2 \overline{\mu}^2 + k_3 \overline{\mu}^3 \tag{6}$$

where k_1, k_2, k_3 are constants and:

$$\overline{\mu} = \frac{\mu - \mu_{lock}}{1 + \mu_{lock}} \tag{7}$$

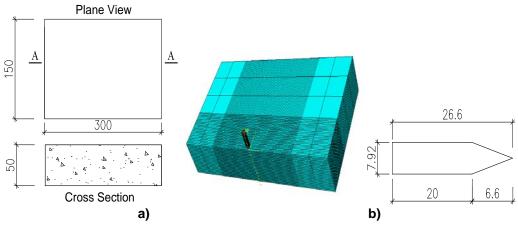where μ_{lock} is the locking volumetric strain.

In this paper, the material model for UHPFRC and HSC panel is the Holmquist-Johnson-Cook model. The material model for deformable steel projectile is the Johnson-Cook model. The material parameters for UHPFRC panel, HSC panel and steel projectile are shown in Table 1, 2. Fig. 1 shows the geometry configurations of the panel, 3D mesh model and the steel projectile. The steel deformable projectile has 8 g of mass and a length of 26.6 mm, 7.92 mm in diameter and is modeled as a deformable element at velocity 540 m/s. The UHPFRC and HSC panel has dimensions of 300 mm × 150 mm × 50 mm, and is meshed using 8-node hexahedron solid elements in ABAQUS explicit software.
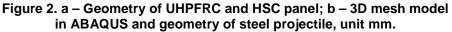
Table 1. The material parameters for UHPFRC and HSC panel.

Variable	Description	UHPFRC	HSC
ρ (Ton/mm^3)	Density	$2.55e^{-9}$	$2.27e^{-9}$
G (MPa)	Shear Modulus	18457	18457
C (MPa)	Strain Rate Law Constant	0.01209	0.01209
A	Failure Surface Constant	0.0017345	0.0075412
T (MPa)	Maximum Allowable Tensile Pressure	6.8946	4.3780
P_{lock} (MPa)	Equation of State Constant	792.88	640.46
μ_{lock}	Locking volumetric strain	0.10094	0.13814
P_{crush} (MPa)	Pressure arising in a uniaxial compression test	172.37	60.60
μ_{crush}	Volumetric strain in a compression test	0.00781	0.00683811
k_1(MPa)	Equation of State Constant	7919.2	6429.9
k_2(MPa)	Equation of State Constant	−29206	−47138.6
k_3(MPa)	Equation of State Constant	187100	255724.2
D_1	Damage constant	0.00040598	0.000311742

Table 2. The material parameters for deformable steel projectile.

Variable	Description	UHPFRC
ρ (Ton/mm³)	Density	$7.86e^{-9}$
G (MPa)	Shear Modulus	$8.18e^4$
E (MPa)	Elastic modulus	$20.9e^4$
PR	Poisson's ratio	0.28
A (MPa)	Yield stress	$7.92\,e^2$
B (MPa)	Hardening constant	$5.1e^2$
C	Strain rate constant	0.014
EPSO (s⁻¹)	Ref. strain rate	1
Failure parameter	D1	0.05
Failure parameter	D2	3.44
Failure parameter	D3	−2.12
Failure parameter	D4	0.002
Failure parameter	D5	0.61

**Figure 2. a – Geometry of UHPFRC and HSC panel; b – 3D mesh model
in ABAQUS and geometry of steel projectile, unit mm.**

A three-dimensional eight-node reduced integration (C3D8R) element was adopted with a 2 mm × 2 mm × 2 mm mesh at the impact location, and 15 mm × 15 mm × 15 mm mesh in the outer region. With the aim to save computational costs and due to the symmetry of the model, half of the UHPFRC panel and projectile is considered. The projectile is meshed with 8-node hexahedron solid elements, with the mesh size of 0.5 mm.

3. Results and Discussion

The pressure distribution of the UHPFRC and High Strength Concrete panel during the impact process are shown in Fig. 3.
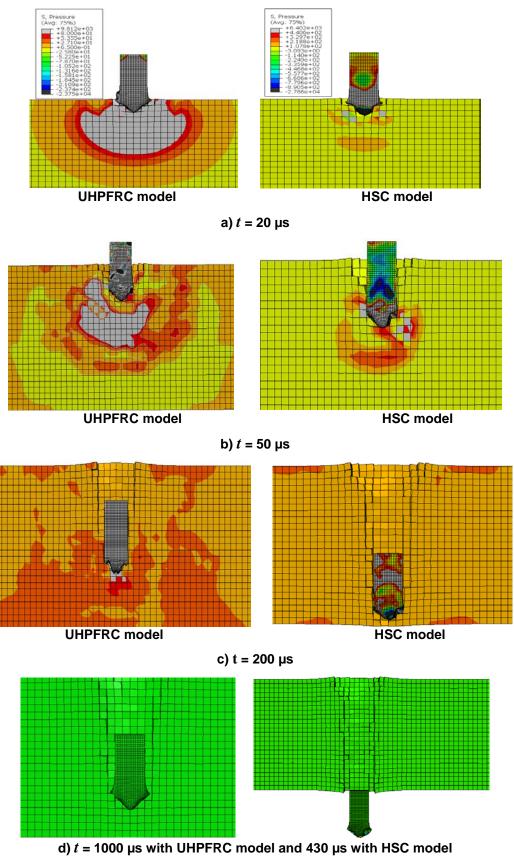
UHPFRC model   **HSC model**

a) t **= 20 μs**

UHPFRC model   **HSC model**

b) t **= 50 μs**

UHPFRC model   **HSC model**

c) t = 200 μs

d) t **= 1000 μs with UHPFRC model and 430 μs with HSC model**

Figure 3. Pressure distribution of model in time step, unit MPa.

At the time after the impact (20 μs and 50 μs), pressure in the UHPFRC and HSC panel reached the highest value and concentrated around the projectile head and the crater. The highest stresses in UHPFRC panel and HSC panel is 9812 MPa and 6402 MPa, respectively. However, compared to HSC material, pressure in the UHPFRC dispersed faster in the larger region. In HSC panel, the projectile was still embedded in panel from 0 μs to 430 μs and HSC panel was perforated by the projectile at t = 430 μs.

Projectile movement speed through the HSC panel was faster than in UHPFRC panel. Residual velocity of the projectile for the HSC panel model was 110.62 m/s. On the other hand, in the UHPFRC panel, the projectile velocity decreased gradually after impacting. It bounced and moved in the opposite direction at time t = 1000 μs without perforating the panel. Based on these results, compared to HSC material, UHPFRC can more effectively absorb the impact energy and reduce the velocity of the projectile.
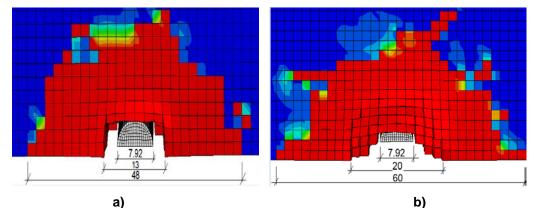

a) b)

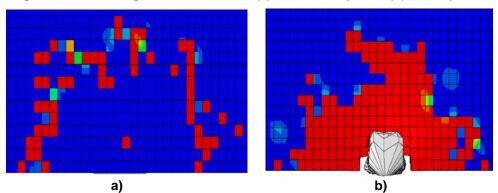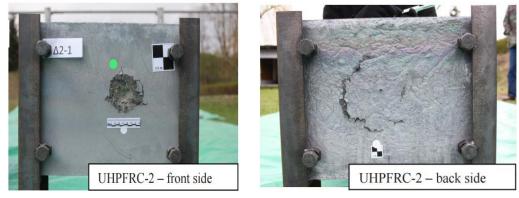**Figure 4. The damage in the front side (a) – UHPFRC panel; (b)– HSC panel.**

a) b)

Figure 5. The damage in the back side (a) – UHPFRC panel; (b) – HSC panel.

UHPFRC-2 – front side UHPFRC-2 – back side

**Figure 6. The experimental result of Radoslav Sovják et al.
with UHPFRC Slab Subjected to Deformable Projectile Impact.**

Table 3. Results after the impact.

Description	UHPFRC	HSC
Projectile	Was stuck	Passed through panel entirely
Residual velocity of Projectile (m/s)	110.62	0
Hole diameter (mm)	13	20
Crater diameter (mm)	48	60
Penetration depth (mm)	42	50

Mai, V.C., Luu, X. B., Nguyen, V.T

Damage state in the front side and backside of UHPFRC and HSC panels is shown in Figs 4-5 and Table 3 The damage variable had a value of 1.0 and 0.0, when the material was totally damaged (featured in red color) and undamaged, respectively. In the front side of UHPFRC and HSC panel, the damage started to initiate at the impact region with an expansion of the fracture around this region. As seen on the front side of the UHPFRC and HSC panel, the hole formed after the impaction was slightly larger than the projectile diameter – 7.92 mm (13 mm in UHPFRC panel and 20 mm in HSC panel). However, the crater (totally damaged region) is about 6 times larger than projectile diameter with the UHPFRC panel and 7.6 times larger with HSC panel, respectively. On the other hand, comparing the hole and crater in UHPFRC and HSC panel, the UHPFRC panel shows a smaller hole diameter (by 35 %) and crater diameter (by 20 %) than the HSC panel. There was no serious damage in the back side of UHPFRC panel. These results are basically similar to the experiments that Radoslav Sovják et. al took with the UHPFRC slabs subjected to deformable projectile impact. UHPFRC material can effectively reduce the damage of impact action.
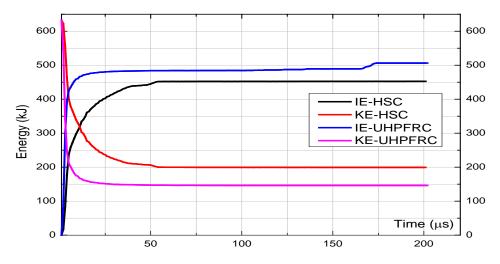

Figure 7. Kinetic energy (KE) of the projectile and internal energy (IE) of panel.

Fig. 7 shows the kinetic energy (KE) of the projectile and the internal energy of panel model (IE) under the 540 m/s of impact velocity. The kinetic energy of the projectile gradually decreased when the projectile penetrating the panel. However, the kinetic energy of the projectile in UHPFRC model (KE-UHPFRC) decreased faster with greater reduction compared to the kinetic energy of the projectile in HSC model (KE-HSC), whereas the internal energy of UHPFRC model (IE-UHPFRC) increased faster than the internal energy of HSC model (IE-HSC). These results should be attributed to the higher energy absorption capacity of the UHPFRC material.
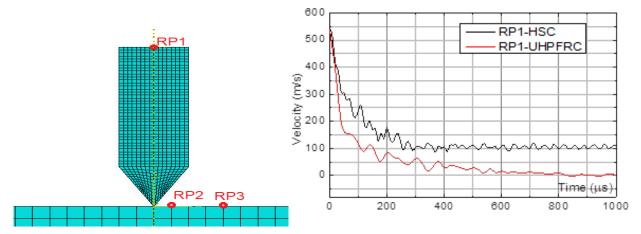

Figure 8. a – Reference points of the model; b – Velocity of RP1 in the projectile.

To evaluate the velocity and acceleration of the model during the impact process, some reference points on the model are chosen, as shown in Fig. 8a.
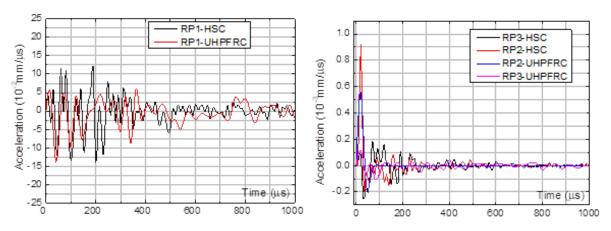
Figure 9. Acceleration of the RP1 in projectile and RP2, RP3 in panel.

Fig. 8b shows the initial velocity of the projectile was 540 m/s, which decreased after the penetration of the HSC panel at 430 µs. The velocity of the projectile started to become stable, which is due to the full penetration of the projectile into the HSC panel. However, projectile movement speed through the UHPFRC panel was slower than in HSC panel. After the impact, the projectile velocity decreased gradually and was close to zero after 1000 µs. Compared to HSC material, it can be clearly seen that UHPFRC material can effectively reduce the velocity of projectile.

From Fig. 9a, it can be noticed that the acceleration of RP1 in the projectile of the UHPFRC panel and HSC panel fluctuated at the beginning of the impact. Then, the acceleration of the projectile was close to zero. In Fig. 9b, the acceleration of RP2 and RP3 in the UHPFRC panel was smaller than the HSC panel. This result indicates that damage in HSC was serious than the UHPFRC panel.

4. Conclusions

This research presents the numerical simulation of the UHPFRC panel subjected to high velocity impact. The result of UHPFRC impact model was compared with the results of HSC impact model. The UHPFRC and HSC material was modeled using the Holmquist-Johnson-Cook model and the steel projectile was simulated as a deformable element by Johnson-Cook model. Analyses of the internal energy of the model and the kinetic energy of the steel projectile were conducted. The variations in velocity and acceleration of the projectile and UHPFRC panel, as well as the pressure, were also calculated. From the results addressed in this research, the following conclusions are drawn:

1. The kinetic energy of the projectile was shown to decrease and when the projectile penetrates into the UHPFRC and HSC panel, the panel tended to absorb the energy of the projectile. It was clearly that UHPFRC has much greater resistance to impact loading compared to HSC also in terms of reducing velocity of projectile and absorbing energy efficiently. Moreover, UHPFRC can reduce the crater and scabbing dimensions on the concrete plate, which decreased the mass loss significantly.

2. Holmquist-Johnson-Cook model can be successfully utilized to simulate the process of UHPFRC under high velocity impact of rigid projectile.

3. Through numerical simulations, the design of new protective structures using UHPFRC material and numerical simulation against high-velocity impact in industrial accidents or explosion generated fragments, can be undertaken. However, to avoid perforation and serious damage to the model, parameters like the thickness of the panel, properties of the UHPFRC are important and should be carefully considered.

5. Conflict of Interests

The authors declare that there is no conflict of interests regarding the publication of this paper.

References

1. Wang, D., Shi, C., Wu, Z., Xiao, J., Huang, Z., Fang, Z. A review on ultra high performance concrete: Part II. Hydration, microstructure and properties. Construction and Building Materials. 2015. 96. Pp. 368–377. https://doi.org/10.1016/j.conbuildmat.2015.08.095

2. Shi, C., Wu, Z., Xiao, J., Wang, D., Huang, Z., Fang, Z. A review on ultra high performance concrete: Part I. Raw materials and mixture design. Construction and Building Materials. 2015. 101. Pp. 741–751. https://doi.org/10.1016/j.conbuildmat.2015.10.088

3. Mai, V.-C., Nguyen, T.-C., Dao, C.-B. Numerical simulation of ultra-high-performance fiber-reinforced concrete frame structure under fire action. Asian Journal of Civil Engineering. 2020. 21. https://doi.org/10.1007/s42107-020-00240-4

4. Yoo, D.Y., Banthia, N. Mechanical properties of ultra-high-performance fiber-reinforced concrete: A review. Cement and Concrete Composites. 2016. 73. Pp. 267–280. https://doi.org/10.1016/j.cemconcomp.2016.08.001

5. Wu, Z., Shi, C., He, W., Wang, D. Static and dynamic compressive properties of ultra-high performance concrete (UHPC) with hybrid steel fiber reinforcements. Cement and Concrete Composites. 2017. 79. Pp. 148–157. https://doi.org/10.1016/j.cemconcomp.2017.02.010

6. Buttignol, T.E.T., Sousa, J.L.A.O., Bittencourt, T.N. Ultra High-Performance Fiber-Reinforced Concrete (UHPFRC): a review of material properties and design procedures, Revista IBRACON de Estruturas e Materiais. 2017. 10. Pp. 957–971. https://doi.org/10.1590/s1983-41952017000400011

7. Azmee, N.M., Shafiq, N. Ultra-high performance concrete: From fundamental to applications, Case Studies in Construction Materials. 2018. 9. https://doi.org/10.1016/j.cscm.2018.e00197

8. Mai, V.-C., Vu, N.-Q., Pham, H., Nguyen, V.-T. Ultra-High Performance Fiber Reinforced Concrete Panel Subjected to Severe Blast Loading. Defence Science Journal. 2020. 70. Pp. 603–611. https://doi.org/10.14429/dsj.70.15835

9. Farnam, Y., Mohammadi, S., Shekarchi, M. Experimental and numerical investigations of low velocity impact behavior of high-performance fiber-reinforced cement based composite. International Journal of Impact Engineering. 2010. 37. Pp. 220–229. https://doi.org/10.1016/j.ijimpeng.2009.08.006

10. Meng, W., Valipour, M., Khayat, K.H. Optimization and performance of cost-effective ultra-high performance concrete. Materials and Structures/Materiaux et Constructions. 2017. 50. https://doi.org/10.1617/s11527-016-0896-3

11. Pham, T.M., Hao, H. Impact Behavior of FRP-Strengthened RC Beams without Stirrups. Journal of Composites for Construction. 2016. https://doi.org/10.1061/(ASCE)CC.1943-5614.0000671

12. Li, J., Wu, C., Hao, H. An experimental and numerical study of reinforced ultra-high performance concrete slabs under blast loads. Materials and Design. 2015. 2015. 82. Pp. 64–76. https://doi.org/10.1016/j.matdes.2015.05.045

13. Xu, J., Wu, C., Xiang, H., Su, Y., Li, Z.X., Fang, Q., Hao, H., Liu, Z., Zhang, Y., Li, J. Behaviour of ultra high performance fibre reinforced concrete columns subjected to blast loading. Engineering Structures. 2016. 118. Pp. 97–107. https://doi.org/10.1016/j.engstruct.2016.03.048

14. Yoo, D.Y., Banthia, N. Mechanical and structural behaviors of ultra-high-performance fiber-reinforced concrete subjected to impact and blast. Construction and Building Materials. 2017. 149. Pp. 416–431. https://doi.org/10.1016/j.conbuildmat.2017.05.136

15. Mai, V.-C., Vu, N.-Q. Assessment of Dynamic Response of 3D Ultra High Performance Concrete Frame Structure under High Explosion Using Johnson-Holmquist 2 Model. KSCE Journal of Civil Engineering. 2020. 00. Pp. 1–11. https://doi.org/10.1007/s12205-020-1373-7

16. Erzar, B., Pontiroli, C., Buzaud, E. Ultra-high performance fibre-reinforced concrete under impact: Experimental analysis of the mechanical response in extreme conditions and modelling using the Pontiroli, Rouquand and Mazars model. Philosophical Transactions of the Royal Society A: Mathematical, Physical and Engineering Sciences. 2017. 375. https://doi.org/10.1098/rsta.2016.0173

17. Sovják, R., Vavřiník, T., Máca, P., Zatloukal, J., Konvalinka, P., Song, Y. Experimental investigation of ultra-high performance fiber reinforced concrete slabs subjected to deformable projectile impact. Procedia Engineering. 2013. 65. Pp. 120–125. https://doi.org/10.1016/j.proeng.2013.09.021

18. Kravanja, S., Sovják, R. Ultra-high-performance fibre-reinforced concrete under high-velocity projectile impact. Part I. experiments. Acta Polytechnica. 2018. 58. Pp. 232–239. https://doi.org/10.14311/AP.2018.58.0232

19. Lai, J., Yang, H., Wang, H., Zheng, X., Wang, Q. Properties and modeling of ultra-high-performance concrete subjected to multiple bullet impacts. Journal of Materials in Civil Engineering. 2018. 30. Pp. 1–11. https://doi.org/10.1061/(ASCE)MT.1943-5533.0002462

20. Holmquist, T.J., Johnson, G.R., Cook, W.H. A computational constitutive model for concrete subjected to large strains, high strain rates, and high pressures. Proc 14th International Symposium on Ballistics, Quebec, 1993.

Contacts:

Viet-Chinh Mai, maivietchinhce@gmail.com

Xuan-Bach Luu, xuanbachmta@gmail.com

Van-Tu Nguyen, nguyentu@lqdtu.edu.vn